Light invariant, efficient, multiple band gap AlGaAs/Si/metal hydride solar cell

S. Licht[a] and B. Wang
Department of Chemistry, Technion–Israel Institute of Technology, Haifa 32000, Israel

T. Soga and M. Umeno
Nagoya Institute of Technology, Gokiso-Cho, Showa-ku, Nagoya 466, Japan

(Received 14 December 1998; accepted for publication 3 May 1999)

Electronic and ionic charge transfer provides a basis for composite semiconductor/electrolyte systems featuring simultaneous solar/electrical conversion and solar energy storage. This cell contains both multiple band gap and electrochemical storage, and provides a nearly constant energetic output in illuminated or dark conditions. Multiple semiconductor band gaps can enhance the energetics of this interaction. The cell combines bipolar AlGaAs ($E_g=1.6$ eV) and Si ($E_g=1.1$ eV) and AB_5 metal hydride/NiOOH storage, and generates a light variation insensitive potential of 1.2–1.3 V at total (including storage losses) solar/electrical energy conversion efficiency of 18.1%. © *1999 American Institute of Physics.* [S0003-6951(99)01826-4]

Whereas electrical needs are largely continuous, clouds and darkness dictate that photovoltaic solar cells have an intermittent output. Photoelectrochemical solar cells (PECs) can generate not only electrical but also electrochemical energy, generating an output insensitive to daily variations in illumination.[1–3] In this study, the first multiple band gap solar cell to combine electrical conversion and storage of solar energy is investigated.

In our recent model,[4] the energetics of twelve distinct multiple band gap[5–9] photoelectrochemical solar cell (MBPEC) configurations were introduced. The various configurations comprised either Schottky or ohmic interfacial electrolyte/semiconductor junctions, utilized either multiple (bipolar) or single (inverted) photon events, and included pathways for optical conversion with or without energy storage.[4] We have recently presented experimental results of a variety of regenerative MBPECs, operating in both bipolar[10] and inverted,[11] modes at solar energy conversion efficiencies approaching 20%, but not capable of energy storage.

Each of the distinct bipolar schemes (Schottky, direct ohmic, indirect ohmic, and with or without storage) are represented in Fig. 1, and comprise a two photon/one electron photoelectrochemical process ($2h\nu \rightarrow e^-$), which may be generalized for an *n* band gap configuration, to an *n* photon process ($nh\nu \rightarrow e^-$). The wide ''*w*'' and small ''*s*'' band gap layers are denoted with respective valence and conduction bands, E_V and E_C, and band gap $E_{Gw}=E_{Cw}-E_{Vw}$, or $E_{Gs}=E_{Cs}-E_{Vs}$. In each of the photocathodic bipolar band gap energy schemes represented in Fig. 1, light shown incident from the left-hand side, first enters the wide band gap layer in which more energetic photons are absorbed; less energetic photons are transmitted, and are absorbed by the small band gap layer. Light of greater than band gap energy, E_{Gw}, drives electron hole pair excitation, the space charge layer inhibits charge recombination, driving the photoexcited electron, e^-*, at photocurrent, j_{photo}, for the *p*-type (wide band gap) conduction band into the quasi-Fermi level of the *n*-type wide band gap layer. Continuing towards the right-hand side in the scheme, charge excited by the wide band gap photon ($h\nu > E_{Gw}$), enters the small band gap layer, where further stimulation, such as to e^-**, occurs by longer wavelength ($h\nu > E_{Gs}$) light. In both Schottky, or *pn*-ohmic schemes, the subsequent space charge field minimizes recombination, driving e^-** through the small band gap semiconductor, facilitating charge transfer to the electrolyte. The photodriven charge sustains reduction at the cathode electrolyte/interface, and drives extractable work through the external load, R_{load}. The generated bipolar MBPEC photovoltage, V_{photo}, is the sum of the potentials of the individual band gap layers, and is constrained by the saturation current through, j_0, through Schottky, or *pn* junctions. This yields a maximum power point photopotential, $V_{p\max}$, less than 60% of the band gap in efficient devices.[12]

Electrochemical energy storage can occur at $E_{\text{redox}}=E_{A+/A}-E_{B/B+}$, as indicated in the left bottom portion of Fig. 1. During illumination of this bipolar storage MBPEC, the charging potential for storage occurs minus cathodic and anodic polarization losses, η:

$$V_{\text{charging}}(\text{light})=(nkT/e)(\ln[1+j_{\text{photo}}/j_{o-w}] \times x[1+j_{\text{photo}}/j_{o-s}])-\eta_{\text{cathode}}+\eta_{\text{anode}}, \quad (1)$$

which must generate a potential greater than the redox storage potential: $E_{B/B+}-E_{A+/A}+\eta_{\text{cathode}}-\eta_{\text{anode}}$. In the absence of illumination, the cell potential is constrained by the redox discharge potential:

$$V_{\text{load}}(\text{dark})=E_{B/B+}-E_{A+/A}-\eta_{\text{cathode}}+\eta_{\text{anode}}. \quad (2)$$

The balancing of the energetics of the solar conversion and storage capacity processes are critical for high efficiency and successful rechargability. A complex energetic challenge exists to choose bipolar band gaps with a combined maximum power point voltage tuned to a high capacity quasireversible storage redox couple potential, in a system also providing efficient solar to electrical energy conversion (high fill factor, open circuit photopotential, and short circuit photocurrent). In a bipolar MBPEC minimization of defects between successive semiconductor layers is critical to mini-

[a]Electronic mail: chrlicht@techunix.technion.ac.il

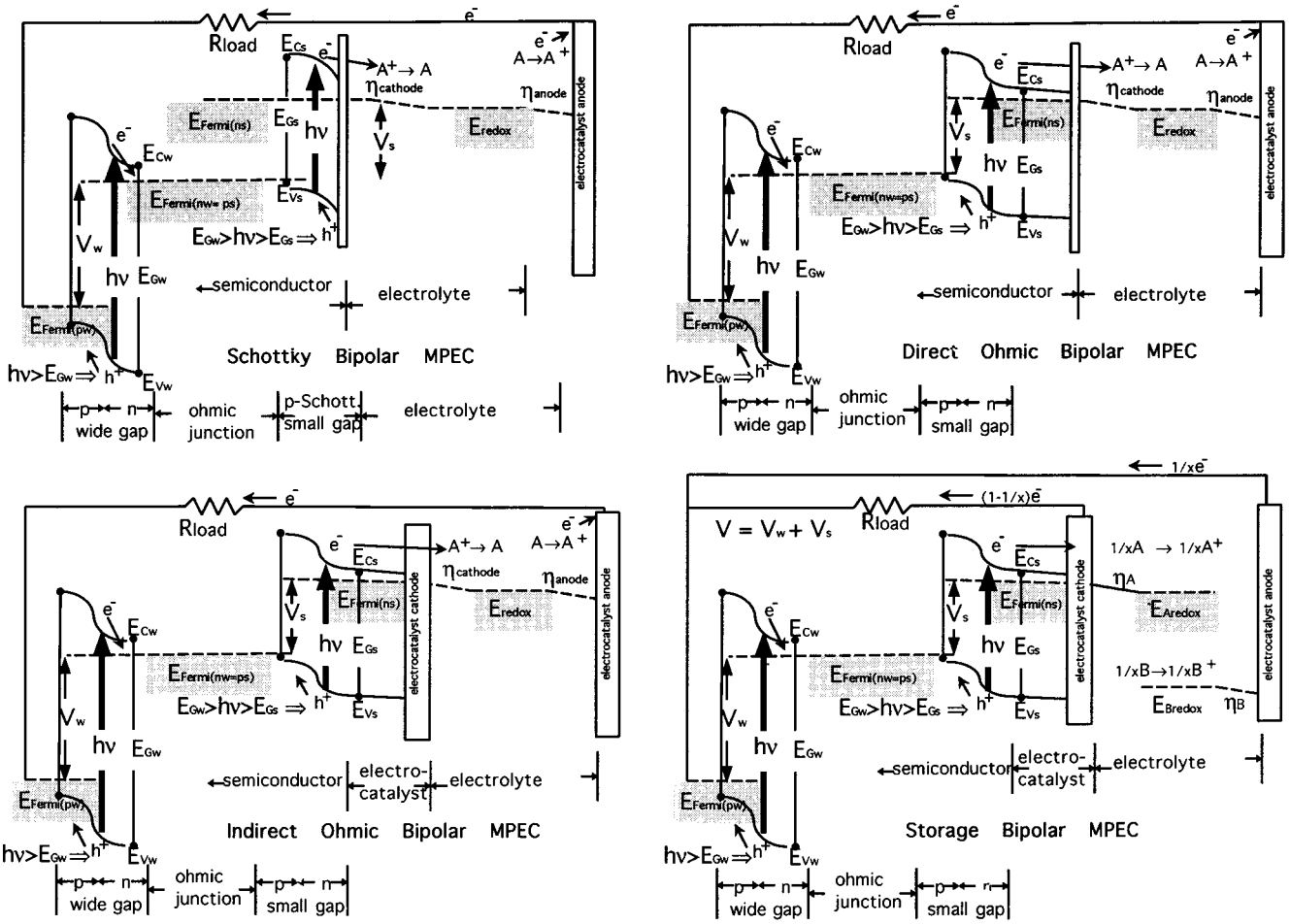

FIG. 1. Energy diagrams for bipolar multiple band gap photoelectrochemistry. Elements of the Schottky or ohmic and direct or indirect semiconductor/electrolyte interface, are shown as well as regenerative and storage modes. Top left side: Schottky regenerative bipolar MBPEC; note that is both a solid state *pn* junction and a Schottky junction between solid *p* type and the electrolyte. Top right side: direct ohmic regenerative bipolar MBPEC; note that there are two solid state *pn* junctions, as well as a direct junction between semiconductor and liquid electrolyte. Bottom left side: bipolar indirect ohmic regenerative MBPEC; note that there are two solid state *pn* junctions, as well as an electrocatalyst situated between the semiconductor and liquid electrolyte. Bottom right: bipolar band gap indirect ohmic storage MBPEC; note the storage potential is the difference between the two electrochemical redox couples A/A^+ and B/B^+.

mize dark current, provide ohmic contact without light absorption loss, and maximize cell efficiency. The multiple band gap bipolar storage solar cell, as shown in the bottom right of Fig. 1, generates a stable output even under dark conditions. This is better illustrated in the schematic Fig. 2, which summarizes the components of an experimentally investigated multiple band gap bipolar storage solar cell. Current flow through the load is in a single direction both in illuminated (shown) and dark (not shown) conditions. Upon illumination, two photons generate each electron, a fraction of which drives a load, while the remainder $(1/xe^-)$ charges the storage redox couple. Without light, the potential falls below E_{redox}, the storage couple spontaneously discharges. This dark discharge is directed through the load, rather than through the multijunction semiconductor's high dark resistance, via electrochemical storage processes such as MH oxidation and NiOOH reduction:

$$\text{MH}+\text{OH}^- \rightarrow \text{M}+\text{H}_2\text{O}+e^-; \quad E=-0.8 \text{ V vs } \text{H}_2; \tag{3}$$

$$\text{NiOOH}+\text{H}_2\text{O}+e^- \rightarrow \text{Ni(OH)}_2+\text{OH}^-;$$

$$E=0.4 \text{ V vs } \text{H}_2. \tag{4}$$

This NiOOH/MH metal hydride storage process is ideal for the AlGaAs/Si due to the excellent match of the storage and photocharging potentials. $V_{\text{storage}}=1.2 \text{ V} + \eta_{\text{charging}}$, while from Eq. (1), $V_{p\max}(\text{AlGaAs/Si})<1.5$ V, using $E_{\text{G–AlGaAs}}=1.6$ eV and $E_{\text{G–Si}}=1.1$ eV. In addition, MH has a

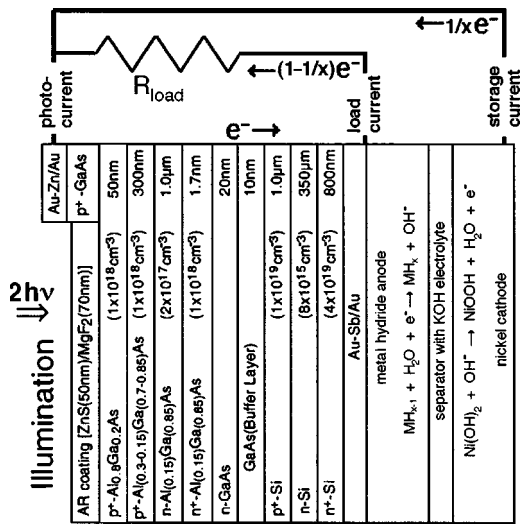

FIG. 2. Schematic representation of the bipolar gap AlGaAs/Si/MH/NIOOH conversion and storage solar cell.

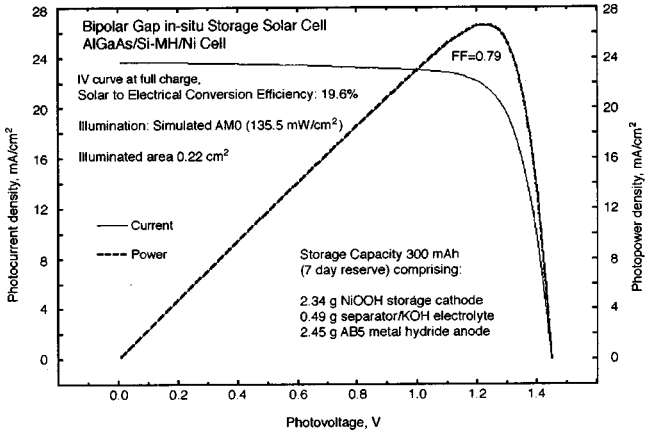

FIG. 3. Photoconversion current and power characteristics of the AlGaAs/Si/MH/NiOOH MBPEC solar cell under fully charged AM0 conditions.

high energy storage capacity >60 Wh/kg, and high quasireversibility providing>500 charge/discharge cycles.[13]

The AlGaAs/Si components in Fig. 2 are prepared by conventional epitaxial growth atmospheric pressure metalorganic chemical vapor deposition.[14–17] The bottom layer consists of a p^+-Si/n-Si/n^+-Si multijunction. Antireflection films are layers of MgF_2/ZnS. Au–Zn/Au and Au–Sb/Au are evaporated as contacts on p- and n-type electrodes. The included backwall photoelectrochemical configuration prevents photon absorption losses by the redox layers.[18] High capacity AB_5 MH and NiOOH electrodes were extracted from the Energizer CP8960D cell and used with a 12 M KOH electrolyte.

The cell contains considerable overcharge protection by utilizing an excess anode charge capacity, with $q_{\text{anode}} \approx 1.2 q_{\text{cathode}}$. During overcharge, rather than $Ni(OH)_2$, oxygen is generated at the cathode which diffuses and oxidizes the anode. This steady-state overcharge process is sustainable, and hydrogen is not evolved. Cells were configured with ~7 day storage capacity as detailed in Fig. 3.

Photocurrent and photopower characteristics of the fully charged AlGaAs/Si/MH solar cell were redundantly measured, with a simple resistive load, and also with a potential controlled PINE AFCBP1 bipotentiostat (using a conventional two electrode cell configuration). These measurements were repeated both under outdoor (AM1.5) and simulated AM0 (using an AM0 solar simulator calibrated tungsten halogen lamp) conditions, yielding the same energy conversion efficiency of 19.6%. The AM0 characteristics are summarized in Fig. 3. Under illumination, the charged AlGaAs/Si/MH solar cell exhibits an open circuit potential of 1.45 V, a short circuit photocurrent 24 mA/cm^2, a fill factor of 0.79, and an observed maximum power photopotential, $V_{p\max} = 1.18-1.28$ V, which provides an energetic match for the metal hydride redox couple.

At the locations indicated at the top of Fig. 2, the conversion/storage experiments measured simultaneous photocurrent, load potential, and storage current using National Instruments LABVIEW digitized data acquisition, and utilized the AM0 calibrated light source, diminished by graded diffuse filters simulating daily insolation fluctuations. Figure 4 presents two days operation of the AlGaAs/Si metal hydride storage solar cell driving an external load. Note the

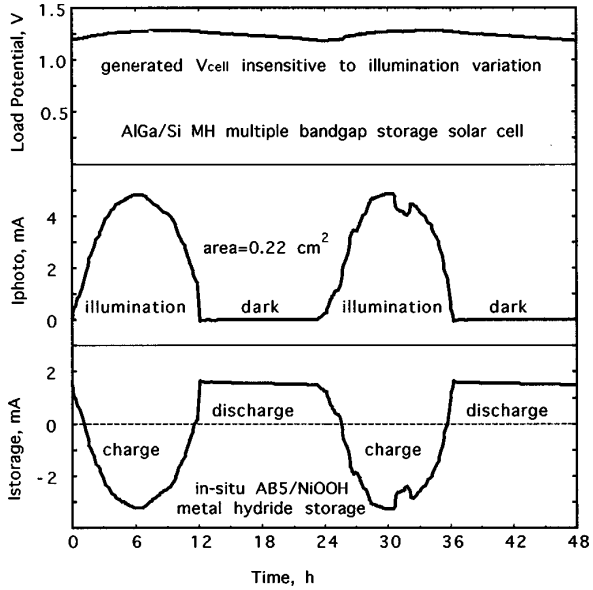

FIG. 4. Two days conversion and storage characteristics of the AlGaAs/Si/MH/NiOOH MBPEC solar cell using a graded diffuse filter varied AM0 illumination.

nearly constant load potential, insensitive to variations in illumination conditions. The overall solar efficiency is determined from a 19.6% photopower efficiency; of this 44% is consumed directly by the load, and the remainder regenerated over the load at 86% energy storage efficiency, to yield an overall solar to electrical conversion efficiency (including both conversion and storage of solar energy) of 18.1%.

The authors are grateful for support by the Israel–Japan Scientific Cooperation, the BMBF Israel-German Cooperation, the Israel Academy and Ministry of Infrastructure, and the Technion and Berman-Shein Solar Fund.

[1] S. Licht, G. Hodes, R. Tenne, and J. Manassen, Nature (London) **326**, 863 (1987).
[2] S. Licht and D. Peramunage, Nature (London) **345**, 330 (1990).
[3] S. Licht, Nature (London) **330**, 148 (1987); Sol. Energy Mater. Sol. Cells **38**, 305 (1995); S. Licht *et al.*, J. Electrochem. Soc. **142**, 840 (1995); **142**, 845 (1995); **142**, 1539 (1995); **142**, 1546 (1995); **142**, L129 (1995); J. Phys. Chem. **100**, 9082 (1996).
[4] S. Licht, O. Khaselev, T. Soga, and M. Umeno, Electrochem. Solid State Lett. **1**, 20 (1998).
[5] C. H. Henry, J. Appl. Phys. **51**, 4494 (1980).
[6] D. J. Friedman, S. R. Kurtz, K. Bertness, A. E. Kibbler, C. Kramer, and J. M. Olsen, Prog. Photovoltaics **3**, 47 (1995).
[7] M. S. Green, K. Emery, K. Bucher, D. L. King, and S. Igari, Prog. Photovoltaics **4**, 321 (1996).
[8] T. Soga, T. Kato, M. Yang, M. Umeno, and T. Jimbo, J. Appl. Phys. **78**, 4196 (1995).
[9] S. Licht, Interface **6**, 34 (1997).
[10] S. Licht, O. Khaselev, P. A. Ramakrishnan, T. Soga, and M. Umeno, J. Phys. Chem. **102**, 2536 (1998).
[11] S. Licht, O. Khaselev, P. A. Ramakrishnan, T. Soga, and M. Umeno, J. Phys. Chem. **102**, 2546 (1998).
[12] R. Memming, in *Photochemical Conversion and Storage of Solar Energy*, edited by E. Pelizzetti and M. Schiavello (Kluwer Academics, Netherlands, 1991), pp. 193–212.
[13] S. R. Ovshinsky, M. A. Fetcenko, and J. Ross, Science **260**, 176 (1993).
[14] T. Soga, T. Kato, M. Umeno, and T. Jimbo, J. Appl. Phys. **79**, 9375 (1996).
[15] H. Shimizu, T. Egawa, T. Soga, T. Jimbo, and M. Umeno, J. Appl. Phys. **31**, L1150 (1992).
[16] M. Yang, T. Soga, T. Jimbo, and M. Umeno, J. Appl. Phys. **33**, 6605 (1994).
[17] T. Soga, M. T. Yang, T. Jimbo, and M. Umeno, Jpn. J. Appl. Phys., Part 1 **35**, 1401 (1996).
[18] S. Licht and F. Farouzan, J. Electrochem. Soc. **142**, 1539 (1995).